Journal of Power Sources Advances 26 (2024) 100138

Contents lists available at ScienceDirect

Journal of Power Sources Advances

journal homepage: www.sciencedirect.com/journal/journal-of-power-sources-advances

On the joint dynamics of potentials and currents in porous electrodes: Model reduction

Keivan Haghverdi [a,b,e,1], Dmitri L. Danilov [c,d,*,1], Grietus Mulder [b,e], Luis D. Couto [b,e], Rüdiger-A. Eichel [a,c]

[a] RWTH Aachen University, D-52074, Aachen, Germany
[b] VITO, Boeretang 200, 2400, Mol, Belgium
[c] Fundamental Electrochemistry (IEK-9), Forschungszentrum Jülich, D-52074, Aachen, Germany
[d] Eindhoven University of Technology, 5600 MB, Eindhoven, the Netherlands
[e] EnergyVille, Thor park 8310, Genk, Belgium

ARTICLE INFO

MSC:
0000
1111

Keywords:
Shooting method
Model order reduction
Porous electrode
Pseudo-two-dimensional
Li-ion battery

ABSTRACT

The dynamic behavior of potentials and currents in porous electrodes is crucial for optimizing the computational speed of lithium-ion battery models. Pseudo-two-dimensional (P2D) models, based on partial differential equations, offer insight but pose computational challenges. P2D equations are tackled with iterative algorithms, like the Newton or the shooting method. Yet, initiating the algorithm with random guesses for solid and electrolyte potentials can cause diverging ionic current values inside the electrolyte phase, increasing the computation time required to converge to the final solution. This study proposes a novel model order reduction using a galvanic pseudo-potential to prevent the occurrence of diverging currents. By sidestepping infinite values for ionic current inside the electrolyte phase, the method streamlines math and speeds up the shooting method used for solving battery model equations.

1. Introduction

Lithium-ion batteries are becoming integral to today's society, by powering various systems including stationary and portable. Their high energy density and rechargeability have transformed how the energy is used and stored. As the demand for clean energy solutions and electric vehicles continues to rise, lithium-ion batteries are a key technology for sustainable progress [1].

Unlocking the potential of lithium-ion batteries necessitates developing and utilizing robust battery models. The pseudo-two-dimensional (P2D) battery model, also known as Doyle-Fuller-Newman (DFN), gathers a system of partial differential equations (PDEs), ordinary differential equations (ODEs), and algebraic equations, and offers a robust framework for analyzing battery dynamics [2–9]. However, the model complexity and its computational demands inherent to solving P2D equations present challenges. In the following sections, one of the challenges related to the convergence of the P2D model solution will be discussed, and a dimension reduction technique designed to enhance the ease of achieving convergence will be introduced in this study.

2. Statement of the problem

The foundation of the battery P2D model lies in its intricate system of equations, covering mass and ionic dynamics within both the solid and the electrolyte phases, and featuring the essential Butler-Volmer equation to describe the kinetic processes. An overview of P2D model equations is presented in Table 2 in Appendix A.

P2D model equations find resolution through iterative solvers like the Newton method or the shooting method. The shooting method transforms a boundary value problem into an initial value problem by making educated guesses for missing initial variables, such as the solid and electrolyte potentials φ_1 and φ_2. It starts with a forward run, often utilizing methods like Euler's or Runge-Kutta, and then iteratively refines these guesses to align the computed ionic current in the electrolyte phase, denoted as i_2, with its specified boundary condition [10]. The iterative refinement process is typically conducted using the bisection method and continues until the desired accuracy in parameter i_2 is attained.

The convergence of iterative algorithms can be jeopardized when

* Corresponding author. Fundamental Electrochemistry (IEK-9), Forschungszentrum Jülich, D-52074, Aachen, Germany.
E-mail address: d.danilov@fz-juelich.de (D.L. Danilov).
[1] K.Haghverdi and D.Danilov have contributed equally to this work.

https://doi.org/10.1016/j.powera.2024.100138
Received 11 January 2024; Accepted 28 January 2024
Available online 29 February 2024
2666-2485/© 2024 The Author(s). Published by Elsevier Ltd. This is an open access article under the CC BY license (http://creativecommons.org/licenses/by/4.0/).

Table 1
Model parameter values and units [17].

Parameters	Values	Units	Description
a	$2.045 \cdot 10^5$	m^{-1}	Particles specific area
i_c^0	$6.328 \cdot 10^{-1}$	$A{\cdot}m^{-2}$	Exchange current density
R	8.314	$J{\cdot}mol^{-1}{\cdot}K^{-1}$	Universal gas constant
T	298	K	Temperature
F	$9.650 \cdot 10^4$	$C{\cdot}mol^{-1}$	Faraday constant
δ	$25 \cdot 10^{-6}$	m	Separator thickness
L	$95 \cdot 10^{-6}$	m	Current collector position
I	-9	$A{\cdot}m^{-2}$	Applied current density
σ_c	$10^{-4} - 10^{-1}$	$S{\cdot}m^{-1}$	Electronic conductivity
κ_c	$10^{-4} - 10^{-1}$	$S{\cdot}m^{-1}$	Ionic conductivity
t_+	0.363	–	Transference number
$c_{0,\text{electrolyte}}$	1300	$mol{\cdot}m^{-3}$	Initial salt concentration in the electrolyte
$U_0(x, T)$	3.386	V	Electrode equilibrium potential

initiating the simulations with random guesses for these potential values, which leads to divergent ionic currents in the electrolyte phase. While techniques like bisection help to refine the range of guesses, the solver may encounter difficulties in breaking out of the loop when faced with infinite values for i_2. The physics-based battery model used in this study is based on the works of Chen et al. [11–13], and Chayambuka et al. [14,15]. It is important to note that the scope of this research extends beyond these specific models and it is a broadly applicable approach for all P2D battery models. The utilized model has encountered this specific issue. For example, exclusively throughout a Constant Voltage (CV) charging phase, there were 4789 occurrences of infinite values encountered by i_2. These instances resulted in 4789 iterations with negligible progress, consequently imposing an increased computational load on the model solution. As an illustrative instance, the parameter list corresponding to the initial values of one of the iterations wherein this issue arises is displayed in Table 1. A similar issue is also observed during constant current (CC) charging, as well as in both constant current and constant voltage discharge phases.

Fig. 1 illustrates examples of infinite values within ionic current in the electrolyte phase i_2 during the iterative process leading to the model solution. Fig. 1a offers a focused view of the first 500 iterations during the CV charging. Complementing this, Fig. 1b presents a comprehensive overview of all the model iterations, revealing not only how frequently infinite values occur but also the continuous sequences of infinite i_2 values in a row during the considered CV charging phase.

An example of the emergence of an infinite value for i_2 at the boundary $x = L$ is presented in Fig. 2. The parameters used for this simulation are presented in Table 1.

In light of these complexities, this study introduces a novel model order reduction technique to circumvent unnecessary iterations and alleviate the computational load associated with the P2D models solved by the shooting method. By introducing a novel approach centered around the concept of a galvanic pseudo-potential, this study addresses the issue of diverging ionic current in the electrolyte phase. This technique streamlines the mathematical framework, offering a more efficient and accurate alternative for handling divergences. The proposed method promises to simplify battery modeling and enhance its computation speed. In the following sections, the intricacies of the proposed model order reduction method are explored, focusing on its formulation and the demonstration of its effectiveness through numerical simulations. Through this research, a pathway is aimed to be provided for refining the accuracy, efficiency, and practicality of battery simulations, thereby contributing to the progress of lithium-ion battery technologies.

3. Model development

To reduce battery modeling complexity, a single porous electrode system, also known as a half cell, has been adopted in the present work. Fig. 3 presents the layout of a porous electrode in a lithium-ion cell, including a separator membrane and a porous electrode filled with electrolyte.

The larger blue solid shapes denote the active electrode particles, and the smaller black circles are the conducting additives. δ represents the thickness of the separator membrane, and L is the thickness of the half cell starting from the negative-electrode/separator interface to the positive electrode current collector. The thickness of the positive porous electrode is equal to $L - \delta$. The negative electrode and separator interface is defined at $x = 0$, and the separator and positive porous electrode interface at $x = \delta$, and the positive electrode/current collector interface at $x = L$.

Consider the cell at some moment of time during battery operation. Suppose that at that moment in time, current density I is applied (variable (t) is skipped for brevity). The system of equations for potentials and currents in both phases can then be written as:

$$i_1 = -\sigma_c \frac{d\varphi_1}{dx}, \tag{1}$$

with boundary conditions

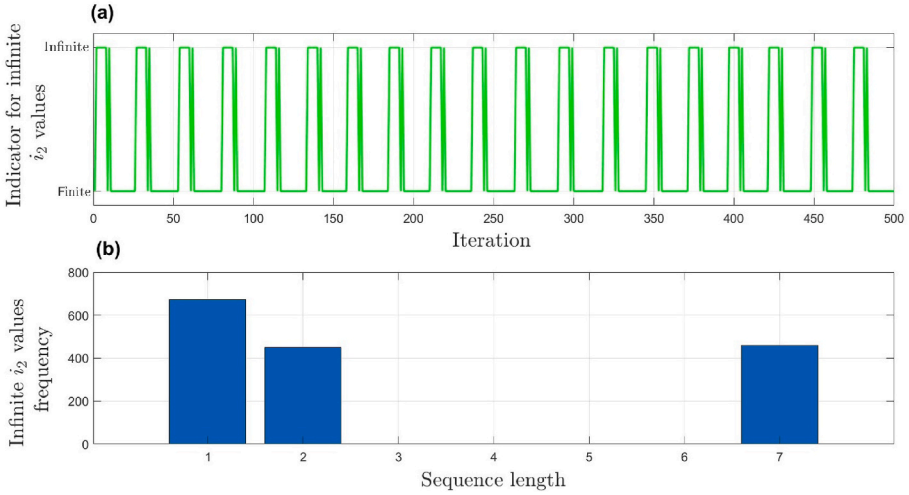

Fig. 1. Frequency of infinite values in ionic current during computational iterations. **(a)** Occurrence of infinite i_2 values within the first 500 of 168684 iterations in a charge/discharge cycle. **(b)** Frequency and sequence length of infinite values out of 168684 iterations in a single charge/discharge cycle.

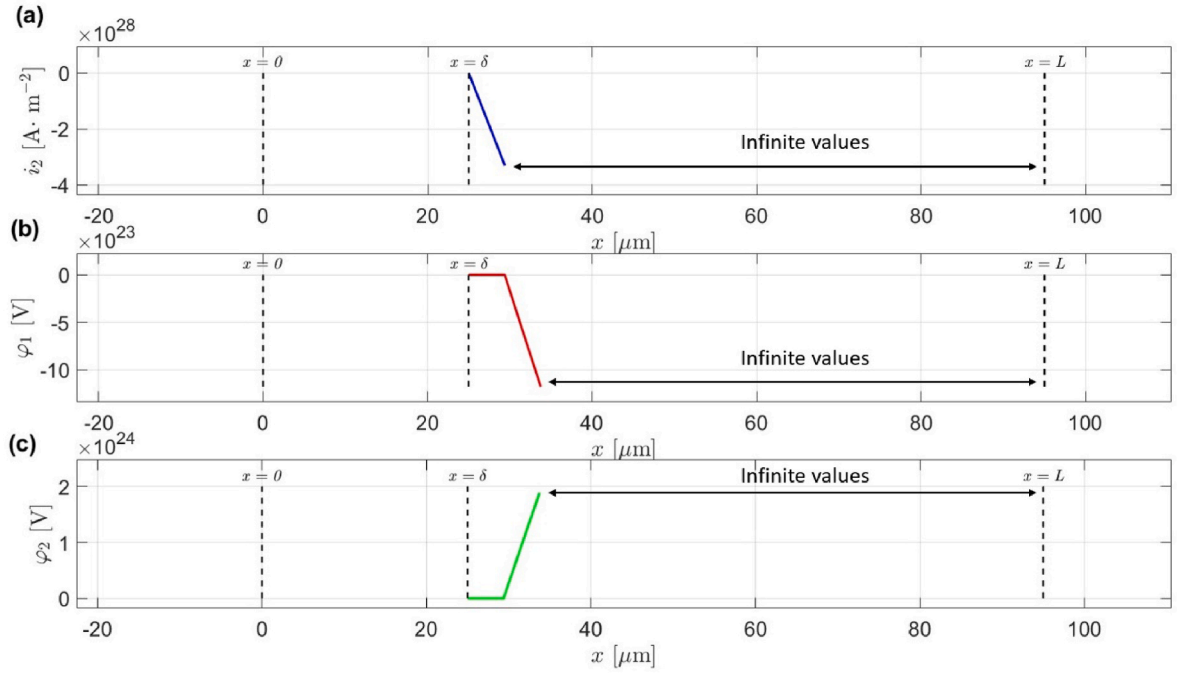

Fig. 2. Illustration of a specific iteration during the CV charging phase, depicting solver encountering infinite values in potential (φ_1, φ_2) and ionic current (i_2). **(a)** i_2 evolution along the x-axis. **(b)** φ_1 evolution along the x-axis. **(c)** φ_2 evolution along the x-axis.

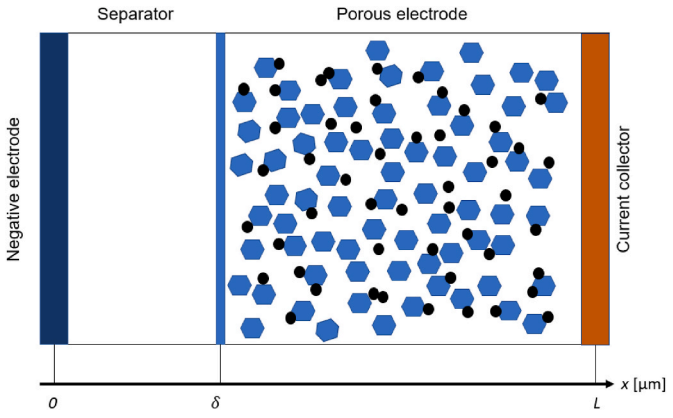

Fig. 3. The layout of a P2D model for a porous electrode in a lithium cell.

$$i_1(\delta) = 0, \quad i_1(L) = I,$$

and

$$i_2 = -\kappa_c \frac{d\varphi_2}{dx} + \frac{2\kappa_c RT}{F}(1 - t_+)\frac{\partial \ln c_2}{\partial x}, \tag{2}$$

with boundary conditions

$$i_2(\delta) = I, \quad i_2(L) = 0,$$

where i_1 and φ_1 represent the electronic current density ($A{\cdot}m^{-2}$) and electrical potential (V) in the porous electrode, i_2 and φ_2 are the ionic current density ($A{\cdot}m^{-2}$) and electrical potential (V) in the electrolyte inside the porous electrode. Note that subscripts 1 and 2 represent the properties of the electrode (solid phase) and electrolyte (liquid phase), respectively. σ_c and κ_c denote the effective electronic conductivity of the electrode and the effective ionic conductivity of the electrolyte ($S{\cdot}m^{-1}$), respectively. The effective conductivity accounts for the actual moving pathways of species in the porous media, for which more detailed information can be found in the literature in the works of Doyle and Fuller et al. [8,9].

The charge transfer between the two phases is described by Eq. (3), known as the Butler-Volmer Equation.

$$\frac{di_2}{dx} = aFj_c = ai_c^0\left[e^{\frac{aF\eta_c^{ct}}{RT}} - e^{-\frac{(1-\alpha)F\eta_c^{ct}}{RT}}\right], \tag{3}$$

where a is the pores specific area (m^{-1}), j_c the reaction rate ($mol{\cdot}m^{-2}{\cdot}s^{-1}$), and i_c^0 is the exchange current density ($A{\cdot}m^{-2}$). Note that j_c becomes the current density when multiplied by the Faraday constant F ($C{\cdot}mol^{-1}$). The charge transfer overpotential η_c^{ct} and its relation with solid and electrolyte phase potential is given in Eq. (4).

$$\eta_c^{ct} = \varphi_1 - \varphi_2 - U_c(c_1^s, T), \tag{4}$$

where U_c is the equilibrium potential of the electrode (V) and c_1^s the Li concentration at electrode particle surface($mol{\cdot}m^{-3}$) with space dependence, I the applied current density ($A{\cdot}m^{-2}$), and R and T are the universal gas constant ($J{\cdot}mol^{-1}{\cdot}K^{-1}$) and absolute temperature (K), respectively. Finally, the conservation of charge results in Eq. (5) illustrated below.

$$i_1 + i_2 = I. \tag{5}$$

For convenience, function G is defined in a way that, $G_{y,z}(\eta) = e^{yz\eta} - e^{-(1-y)z\eta}$, where $y = \alpha$ and $z = \frac{F}{RT}$. Eq. (3) can then be represented by

$$\frac{di_2}{dx} = ai_c^0 G_{\alpha,z}(\varphi_1 - \varphi_2 - U_c(c_1^s, T)). \tag{6}$$

Eliminating i_1 according to Eq. (5) and rearranging equations lead to the following system of ordinary differential equations

$$\frac{d\varphi_1}{dx} = \frac{i_2 - I}{\sigma_c}, \tag{7}$$

$$\frac{d\varphi_2}{dx} = -\frac{i_2}{\kappa_c} + \frac{2RT}{F}(1 - t_+)\frac{\partial \ln c_2}{\partial x}, \tag{8}$$

$$\frac{di_2}{dx} = ai_c^0 G_{\alpha,z}(\varphi_1 - \varphi_2 - U_c(c_1^s, T)). \tag{9}$$

Now subtract Eq. (8) from Eq. (7) and introduce galvanic pseudo-potential $\psi = \varphi_1 - \varphi_2$. The system of Eqs. (7)–(9) then takes the following form

$$\begin{aligned}\frac{d\psi}{dx} &= \frac{i_2 - I}{\sigma_c} + \frac{i_2}{\kappa_c} - \frac{2RT}{F}(1 - t_+)\frac{\partial \ln c_2}{\partial x} \\ &= \frac{\kappa_c + \sigma_c}{\kappa_c \sigma_c} i_2 - \frac{I}{\sigma_c} - \frac{2RT}{F}(1 - t_+)\frac{\partial \ln c_2}{\partial x},\end{aligned} \tag{10}$$

$$\frac{di_2}{dx} = ai_c^0 G_{\alpha,z}(\psi - U_c(c_1^s, T)). \tag{11}$$

It is important to note that the function $(U_c(c_1^s, T))$, which represents the concentration-dependent electrochemical potential, is inherently a function of the spatial coordinate x due to the concentration in the solid phase being dependent on x. This dependence is highlighted by the notation $(U_c(c_1^s(x), T))$. Moreover, it is possible to simplify this expression, particularly when dealing with low overpotentials, especially during the initial stages of the current application. In such cases, the term $(U_c(x, T))$ tends to become spatially uniform and it is effectively transformed into a constant value. This behavior has been discussed in the context of the work of Chen et al. [16], emphasizing the significance of this simplification in understanding the electrochemical processes under specific conditions.

System of Eqs. (10) and (11) has a smaller dimension than the original Eqs. (7)–(9). It is expected that values of ionic current inside the electrolyte phase at the current collector interface will be finite from the very beginning. Eq. (11) has two boundary conditions

$$i_2(\delta) = I, \tag{12}$$

and

$$i_2(L) = 0. \tag{13}$$

The boundary-value problem associated with Eqs. (10)–(13) is systematically tackled by the bisection method or any other root-finding algorithm to iteratively adjust the value of $\psi(\delta)$ within a predefined range of tentative values. This range is initially established using two values, ψ_{low} and ψ_{high}, as initial guesses which are chosen to satisfy the following condition:

$$i_2(\psi_{high}, L) \cdot i_2(\psi_{low}, L) \leq 0. \tag{14}$$

The fulfillment of the condition of Eq. (14) ensures the presence of a root within this initial range of guesses. The fulfillment of this condition is not considered a challenging task. The selection of a range deemed sufficiently wide to encompass the solution is all that needs to be accomplished. Typically, the lithium-ion battery is operated within a specific voltage boundary. That provides a common sense for determining the appropriate size of the range.

A more effective approach to facilitate an efficient range estimation is to do a preliminary shooting method by using a linear approximation of the Butler-Volmer equation shown in Eq. (15).

$$j_c = \frac{i_c^0}{F}\left[e^{\frac{\alpha F \eta_c^{ct}}{RT}} - e^{-\frac{(1-\alpha)F\eta_c^{ct}}{RT}}\right] \approx \frac{i_c^0 \eta_c^{ct}}{RT}. \tag{15}$$

This method, while fast in computation and straightforward, is primarily applicable to scenarios characterized by low overpotential. Despite its inherent limitation, it serves as a reliable initial estimate for the range intended to be explored in the quest to identify the root and solution of our problem. With the help of Eq. (15), an initial range for these guesses for ψ values can be initialized that satisfies Eq. (14). Following the outcomes derived from the preliminary shooting method, a range of values for ψ is defined to serve as the input for our primary shooting method.

The subsequent step is to pinpoint the root of the system of equations by progressively narrowing down this range, employing methods such as bisection. To initiate this process, the solver with the following initial conditions is set as shown in Eq. (16).

$$i_2(\delta) = I, \quad \psi(\delta) = \psi_i. \tag{16}$$

In the first two starting iterations, the guess that is used for the value of ψ is ψ_{high} for the upper limit and ψ_{low} for the lower limit of the specified range. After establishing the initial bisection range, the primary aim is to track the value of $i_2(\psi_i, L)$ with the objective of achieving:

$$|i_2(\psi_i, L) - i_2(L)| < \epsilon. \tag{17}$$

Here, ε serves as a predefined small number acting as the convergence criterion and $i_2(L)$ is equal to zero according to the boundary condition stated in Eq. (13). In other words, when the estimated value of $i_2(\psi_i, L)$ closely approximates the boundary condition value $i_2(L)$ at the current collector location, the correct solution is achieved.

The system of equations represented by Eqs. (10) and (11) exhibits a reduced order compared to the original set of Eqs. (7)–(9). It is anticipated that the values of $i_2(\psi_i, L)$ will remain finite right from the initial stages. That achievement is a direct result of the model order reduction technique explained in this study. Notably, even as φ_1 and φ_2 approach infinity, the difference between them denoted as $\psi = \varphi_1 - \varphi_2$, remains a finite value, guaranteeing that the values of i_2 persist as finite throughout the simulation. This results in avoiding unnecessary iterations around infinite values and overall faster convergence. This model reduction can also be helpful for utilizing better equation-solving methods, not only bisection.

The transition from the original PDE to an ODE becomes apparent through time discretization methods like implicit, explicit, or mixed techniques. As a result, this yields the equations comprising Eqs. (1)–(5). This forms the core of the ODE system given by Eq. (7) through Eq. (9).

In the original model before order reduction, the inherent stiffness of the problem derives from exponential functions within the Butler-Volmer equation. An imprecise initial estimation, if excessively large, has the potential to induce significant magnitudes of i_2. Subsequently, in successive iterations, φ_1 and φ_1 variables might undergo exponential growth. From the definition of pseudopotential ψ it follows that though both φ_1 and φ_2 can grow very large their difference should remain of a moderate magnitude.

This study employs a spatial discretization technique based on the finite difference method as the foundational approach for analysis. Subsequently, the forward Euler method is utilized to iteratively process each discretized point. This combined methodology facilitates effective navigation through the spatial domain and the progression of computations through each iteration. As a result, it provides a robust framework for investigating the dynamics and behaviors within the system under examination. Notably, the new reduced-order model has effectively converted cases that previously yielded infinite values in the earlier model into finite ones.

4. Results and discussion

Table 1 presents the values employed in the simulations shown in Figs. 1 and 2. These values showcase a CV charging scenario of a house-made button cell described in the work of Chen et al. [17].

In the simulations above, the boundary condition $i_2(\delta)$ outlined in Eq. (12) within the separator region is the foundation for the initial conditions during the forward simulation. The outcome of this forward simulation, denoted as $i_2(L, \psi)$ is compared to the boundary condition $i_2(L)$ as depicted in Eq. (13). The criterion for convergence is shown in Eq. (17). When this condition holds, the values have effectively solved the system of differential equations. However, should the inequality not be satisfied, the process will be iterated further by refining the initial approximation for ψ and continuing until convergence.

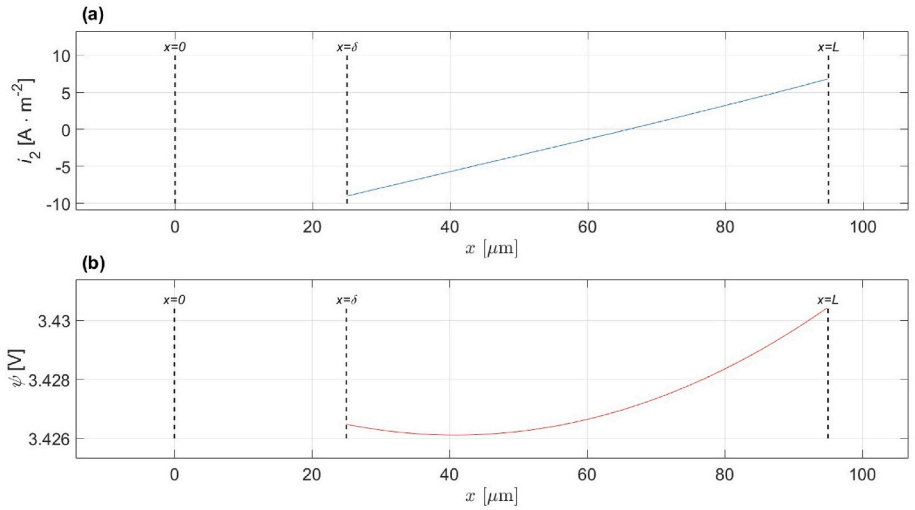

Fig. 4. **(a)** Numerical simulation of i_2 in porous electrode **(b)** Numerical simulation of ψ in the porous electrode.

It is important to note that the proposed model dimension reduction in this study prevents the emergence of infinite ionic current in electrolyte i_2 values at the boundary of the current collector. This achievement arises from eliminating its dependence on distinct potentials within the solid and electrolyte phases, namely φ_1 and φ_2. The visual representation of the simulation outcomes is encapsulated in Fig. 4, showcasing the solution to the system of ordinary differential equations detailed in Eqs. (10) and (11). The same model parameters (see Table 1) as in previous simulations (see Figs. 1 and 2) were used. This time, the proposed reduced order model technique was implemented, and for the same parameters and initial conditions, the values of i_2 do not become infinite during the iteration process.

5. Conclusion

This research provides a valuable way to improve the accuracy, efficiency, and applicability of battery model simulations by addressing a critical challenge in the shooting method. By tackling the issue of diverging ionic currents inside the electrolyte phase, the proposed model order reduction method offers a more robust and expedited approach to studying and optimizing lithium-ion battery systems.

This study streamlines battery behavior modeling by adopting a single porous electrode system. The study introduces the galvanic pseudo-potential ψ, a key concept representing the potential difference between solid and electrolyte phases. This formulation enables the iterative shooting method to avoid infinite values for ionic current in electrolyte i_2, at the interface of the electrode and current collector. This approach not only simplifies the problem but also lays the foundation for advanced equation-solving methods, promising more effective simulation techniques in battery research and development.

CRediT authorship contribution statement

Keivan Haghverdi: Conceptualization, Investigation, Software, Validation, Visualization, Writing – original draft. **Dmitri L. Danilov:** Conceptualization, Methodology, Supervision, Writing – review & editing. **Grietus Mulder:** Conceptualization, Writing – review & editing. **Luis D. Couto:** Conceptualization, Writing – review & editing. **Rüdiger-A. Eichel:** Project administration.

Declaration of competing interest

The authors declare that they have no known competing financial interests or personal relationships that could have appeared to influence the work reported in this paper.

Data availability

Data will be made available on request.

Acknowledgments

Dmitri L. Danilov is supported by the ProMoBis BMBF project (Germany), Grant No. 03ETE046C.

Appendix A. Supplementary data

Table 2
P2D model equations

Name of Equation	Mathematical Equation
Diffusion in particles	$\frac{\partial c_1}{\partial t} = \frac{1}{r^2}\frac{\partial}{\partial r}\left(r^2 D_1 \frac{\partial c_1}{\partial r}\right)$
Kinetics	$i_c^0 = Fk(c_1^{max} - c_1^s)^{\alpha}(c_1^s)^{(1-\alpha)}(c_2)^{\alpha}$ $j = \frac{i_c^0}{F}\left[e^{\frac{\alpha F \eta^{ct}}{RT}} - e^{-\frac{(1-\alpha)F\eta^{ct}}{RT}}\right]$
Mass balance	$\epsilon\frac{\partial c_2}{\partial t} = \frac{\partial}{\partial x}\left(D_2^{eff}\frac{\partial c_2}{\partial x}\right) + aj(1-t_+)$
Potential in solution	$i_2 = -\kappa_c\frac{\partial \varphi_2}{\partial x} + \frac{2\kappa_c RT}{F}(1-t_+)\left(1+\frac{dlnf_{\pm}}{dlnc_2}\right)\frac{\partial lnc_2}{\partial x}$

(*continued on next page*)

Table 2 (*continued*)

Name of Equation	Mathematical Equation
Potential in solid	$i_1 = -\sigma_c \frac{\partial \varphi_1}{\partial x}$
	$i_1 + i_2 = I$
	$Faj = \frac{\partial i_2}{\partial x}$
Battery output voltage	$V_{bat} = \varphi_1\|_{x=L} - \varphi_1\|_{x=0} - IR_f$

References

[1] D. Raimi, E. Campbell, R. Newell, B. Prest, S. Villanueva, J. Wingenroth, Global Energy Outlook 2022: Turning Points and Tension in the Energy Transition, Resources for the Future, Washington, DC, USA, 2022.

[2] J.S. Newman, C.W. Tobias, Theoretical analysis of current distribution in porous electrodes, J. Electrochem. Soc. 109 (12) (1962) 1183.

[3] J. Newman, W. Tiedemann, Porous-electrode theory with battery applications, AIChE J. 21 (1) (1975) 25–41.

[4] R. Darling, J. Newman, On the short-time behavior of porous intercalation electrodes, J. Electrochem. Soc. 144 (9) (1997) 3057.

[5] K. Scott, P. Argyropoulos, A current distribution model of a porous fuel cell electrode, J. Electroanal. Chem. 567 (1) (2004) 103–109.

[6] O. Lanzi, U. Landau, Effect of pore structure on current and potential distributions in a porous electrode, J. Electrochem. Soc. 137 (2) (1990) 585.

[7] S. Szpak, T. Katan, An experimental study of reaction profiles in porous electrodes, J. Electrochem. Soc. 122 (8) (1975) 1063.

[8] M. Doyle, T.F. Fuller, J. Newman, Modeling of galvanostatic charge and discharge of the lithium/polymer/insertion cell, J. Electrochem. Soc. 140 (6) (1993) 1526.

[9] T.F. Fuller, M. Doyle, J. Newman, Simulation and optimization of the dual lithium ion insertion cell, J. Electrochem. Soc. 141 (1) (1994) 1.

[10] M.R. Osborne, On shooting methods for boundary value problems, J. Math. Anal. Appl. 27 (2) (1969) 417–433.

[11] Z. Chen, D.L. Danilov, L.H. Raijmakers, K. Chayambuka, M. Jiang, L. Zhou, J. Zhou, R.-A. Eichel, P.H. Notten, Overpotential analysis of graphite-based li-ion batteries seen from a porous electrode modeling perspective, J. Power Sources 509 (2021) 230345.

[12] Z. Chen, D.L. Danilov, R.-A. Eichel, P.H. Notten, Li+ concentration waves in a liquid electrolyte of li-ion batteries with porous graphite-based electrodes, Energy Storage Mater. 48 (2022) 475–486.

[13] Z. Chen, D.L. Danilov, R.-A. Eichel, P.H. Notten, Porous electrode modeling and its applications to li-ion batteries, Adv. Energy Mater. 12 (32) (2022) 2201506.

[14] K. Chayambuka, G. Mulder, D.L. Danilov, P.H. Notten, Determination of state-of-charge dependent diffusion coefficients and kinetic rate constants of phase changing electrode materials using physics-based models, J. Power Sourc. Adv. 9 (2021) 100056.

[15] K. Chayambuka, G. Mulder, D.L. Danilov, P.H. Notten, A hybrid backward euler control volume method to solve the concentration dependent solid-state diffusion problem in battery modeling, J. Appl. Math. Phys. 8 (6) (2020) 1066–1080.

[16] Z. Chen, D.L. Danilov, R.-A. Eichel, P.H. Notten, Reaction-rate distribution at large currents in porous electrodes, J. Power Sources 581 (2023) 233495.

[17] Z. Chen, D.L. Danilov, R.-A. Eichel, P.H. Notten, On the reaction rate distribution in porous electrodes, Electrochem. Commun. 121 (2020) 106865.